

**Self-Assembly of Single-Chain Nanoparticles from Block Copolymers into Inverse  
Bicontinuous Structures**

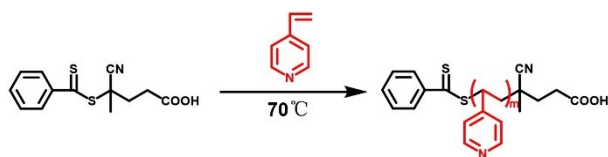
**Yalan Sun, Zichao Deng, Aihua Chen\***

School of Materials Science and Engineering, Beihang University  
No. 37 Xueyuan Road, Haidian District, Beijing 100191, P. R. China

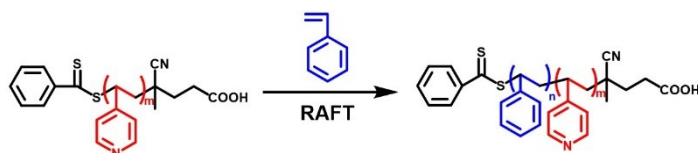
\*Corresponding author.

E-mail: [chenaihua@buaa.edu.cn](mailto:chenaihua@buaa.edu.cn)

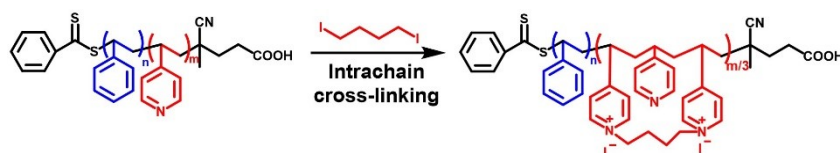
## Synthesis routes of P4VP-CTA, P4VP-*b*-PS, and P4VP(SCNP)-*b*-PS



**Scheme S1.** The synthesis route of P4VP-CTA.



**Scheme S2.** The synthesis route of P4VP-*b*-PS.



**Scheme S3.** The synthesis route of P4VP(SCNP)-*b*-PS.

## Characterization.

**NMR Spectroscopy.**  $^1\text{H}$  NMR spectra were obtained by Bruker DMX Spectrometer (400 MHz) using  $\text{CDCl}_3$  as a solvent.

**Gel Permeation Chromatography (GPC).** The P4VP-*b*-PS and P4VP(SCNP)-*b*-PS were measured on Waters 2410 GPC. The eluent was THF with a flow rate of 1 mL/min. The samples were dissolved in THF, and filtered through 0.22  $\mu\text{m}$  syringe filters. The calibration curves were obtained from PS standards. Some samples were also measured on a system consisted of Wyatt Technology detector, Agilent HPLC pump, and Agilent mixed columns (Plgel 20  $\mu\text{m}$  MIXED-A and PLgel 10  $\mu\text{m}$  MIXED-B). The eluent of DMF with LiBr (0.05 mol/L) was used and the measurements were conducted at 25  $^\circ\text{C}$  with a flow rate of 1 mL/min.

**Dynamic Light Scattering (DLS).** DLS measurements were conducted on the instrument of Shandong Naikete NKT-N9 with a 532 nm He-Ne laser.

**Scanning Electron Microscopy (SEM).** Images were taken using a Tescan Vega3 microscope with an accelerating voltage of 30 kV and a Zeiss SUPRA55 instrument at an accelerating voltage of 10

kV. The dilute dispersion solution was dropped onto a silicon wafer and then sputtered with gold.

**Transmission Electron Microscopy (TEM).** Images were taken using a JEM-2100Plus microscope with an accelerating voltage of 200 kV. The dilute dispersion solution was dropped onto a copper grid.

**Small Angle X-ray Scattering (SAXS).** SAXS measurements were performed on the synchrotron radiation at BL16B1 beamline provided by Shanghai Synchrotron Radiation Facility (SSRF) with a wavelength of 1.24 Å at room temperature.

### **Synthesis of P4VP-CTA via RAFT solution polymerization**

P4VP macromolecular chain transfer agents (macro-CTAs) were synthesized by reversible addition-fragmentation chain transfer (RAFT) solution polymerization (Scheme S1). Typically, 4-VP (0.63 g, 6.0 mmol), CPADB (40.5 mg, 0.1 mmol), and AIBN (1.64 mg, 0.01 mmol) dissolved in 3 mL ethanol were added into a Schlenk flask. After three freeze-pump-thaw cycles, the flask was sealed. The reaction was quenched in liquid nitrogen after 6 h at 70 °C and precipitated in petroleum ether three times. Then the product was dialyzed in ethanol and dried under vacuum. The degree of polymerization of P4VP ( $DP_{P4VP}$ ) is calculated by  $^1H$  NMR (Figure S1) as follows:

$$DP_{P4VP} = \frac{I_d}{I_b} \quad (S1)$$

where  $I_b$  represents the integrated value of the proton peaks originating from the phenyl groups of 4-Cyano-4-(phenylcarbonothioylthio) pentanoic acid (CPADB) (signal b,  $\delta = 7.78-7.90$  ppm);  $I_d$  represents the integrated value of the proton peaks attributed to the pyridine groups of P4VP block (signal d,  $\delta = 8.15-8.65$  ppm).

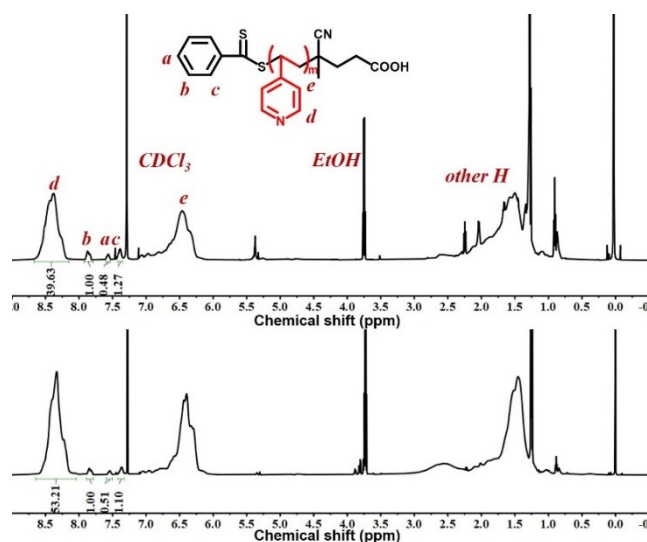


**Figure S1**  $^1\text{H}$  NMR spectra of P4VP<sub>40</sub>-CTA and P4VP<sub>53</sub>-CTA (from top to bottom).

### Synthesis of P4VP-*b*-PS via RAFT dispersion polymerization

The degree of polymerization of PS ( $\text{DP}_{\text{PS}}$ ) is calculated by  $^1\text{H}$  NMR as follows:<sup>1</sup>

$$\frac{I_a}{I_{b+c+d}} = \frac{2 \times \text{DP}_{\text{P4VP}}}{5 \times \text{DP}_{\text{PS}} + 2 \times \text{DP}_{\text{P4VP}}} \quad (\text{S2})$$

where  $I_a$  represents the integrated value of the proton peaks at 8.20-8.60 ppm, originating from the pyridine groups of P4VP block (signal a);  $I_{b+c+d}$  represents the integrated value of the proton peaks at 6.20-7.20 ppm, originating from the phenyl groups of PS block and the pyridine groups of P4VP block. Accordingly, the  $\text{DP}_{\text{PS}}$  is calculated as follows:

$$\text{DP}_{\text{PS}} = \frac{2 \times \text{DP}_{\text{P4VP}} \times \left( \frac{I_{b+c+d+e}}{I_a} - 1 \right)}{5} \quad (\text{S3})$$

Taking P4VP<sub>53</sub>-*b*-PS<sub>499</sub> as an example:

$$\text{DP}_{\text{PS}} = \frac{2 \times \text{DP}_{\text{P4VP}} \times \left( \frac{I_{b+c+d+e}}{I_a} - 1 \right)}{5} = \frac{2 \times 53 \times \left( \frac{24.56}{1} - 1 \right)}{5} \approx 499$$

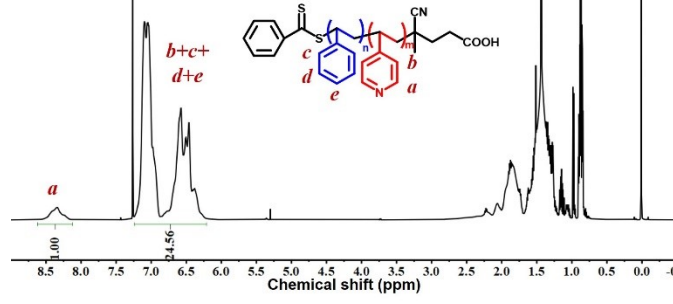


**Figure S2.**  $^1\text{H}$  NMR spectrum of P4VP<sub>53</sub>-*b*-PS<sub>499</sub>.

The volume fraction of the PS block ( $f_{\text{PS}}$ ) is calculated as follows:<sup>2</sup>

$$f_{\text{PS}} = \frac{V_{\text{PS}}}{V_{\text{P4VP}} + V_{\text{PS}}} = \frac{M_{\text{PS}}/\rho_{\text{PS}}}{M_{\text{P4VP}}/\rho_{\text{P4VP}} + M_{\text{PS}}/\rho_{\text{PS}}} \quad (\text{S4})$$

In equation S4,  $V_{\text{P4VP}}$  and  $V_{\text{PS}}$  represent the volumes of P4VP and PS chains respectively;  $M_{\text{P4VP}}$  and  $M_{\text{PS}}$  denote the molecular weights of the P4VP and PS blocks, respectively;  $\rho_{\text{P4VP}}$  represents the density of P4VP, which is about 1.15 g cm<sup>-3</sup>;  $\rho_{\text{PS}}$  represents the density of PS, which is about 1.05 g cm<sup>-3</sup>.

Taking P4VP<sub>53</sub>-*b*-PS<sub>499</sub> as an example:

$$f_{\text{PS}} = \frac{V_{\text{PS}}}{V_{\text{P4VP}} + V_{\text{PS}}} = \frac{M_{\text{PS}}/\rho_{\text{PS}}}{M_{\text{P4VP}}/\rho_{\text{P4VP}} + M_{\text{PS}}/\rho_{\text{PS}}} = \frac{499 \times 104/1.05}{53 \times 105/1.15 + 499 \times 104/1.05} \approx 91.1\%$$

### Preparation and characterization of tadpole-like SCNPs.

The number of DIB ( $x$ ) linked to P4VP is calculated by  $^1\text{H}$  NMR as follows:

$$x = \frac{1}{4} \times \frac{I_f \times 2 \times DP_{\text{P4VP}}}{I_a} \quad (\text{S5})$$

Therefore, the actual CD of SCNPs is calculated by the following equation:

$$\text{CD} = \frac{2x}{DP_{\text{P4VP}}} \times 100\% = \frac{I_f}{I_a} \times 100\% \quad (\text{S6})$$

Taking CD<sub>27%</sub>-P4VP(SCNP)<sub>53</sub>-*b*-PS<sub>569</sub> as an example (Figure S3):

$$x = \frac{1}{4} \times \frac{I_f \times 2 \times DP_{\text{P4VP}}}{I_a} = \frac{1}{4} \times \frac{0.27 \times 2 \times 53}{1} = 7.155$$

$$CD = \frac{2 \times 7.155}{53} \times 100\% = \frac{I_f}{I_a} \times 100\% = \frac{0.27}{1} \times 100\% = 27\%$$

So, this sample can be named CD<sub>27%</sub>-P4VP(SCNP)<sub>53</sub>-*b*-PS<sub>569</sub>.

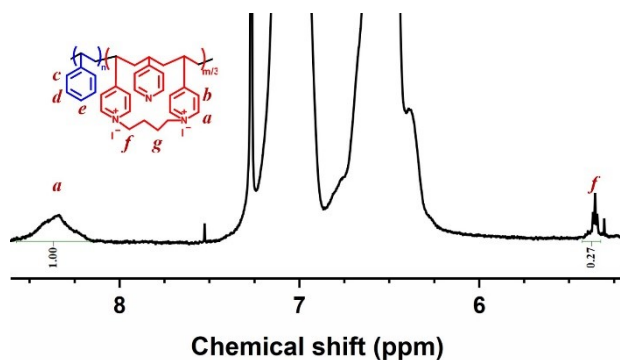


**Figure S3.** <sup>1</sup>H NMR spectrum of CD<sub>27%</sub>-P4VP(SCNP)<sub>53</sub>-*b*-PS<sub>569</sub> prepared in dilute DCM solution.

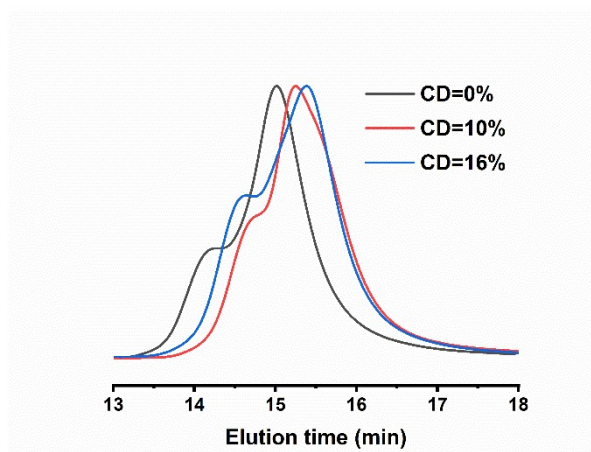


**Figure S4.** GPC traces of P4VP(SCNP)<sub>40</sub>-*b*-PS<sub>512</sub> using DMF as the eluent.

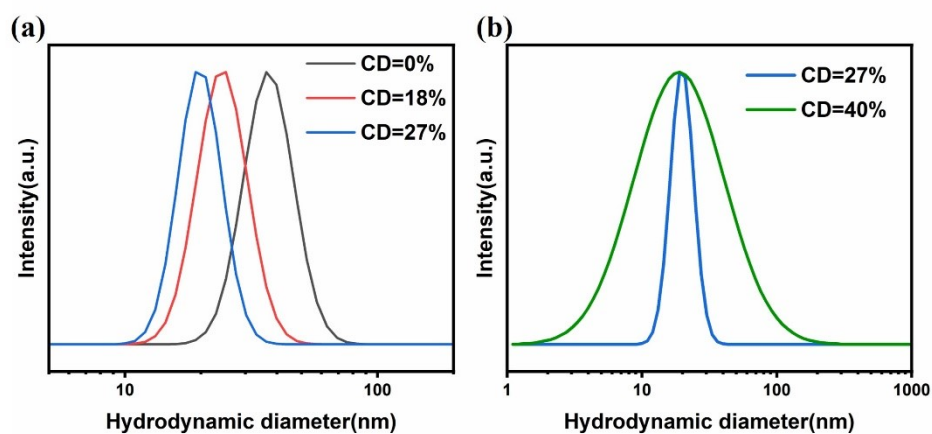


**Figure S5.** (a) DLS curves of P4VP<sub>53</sub>-*b*-PS<sub>569</sub> and P4VP(SCNP)<sub>53</sub>-*b*-PS<sub>569</sub> at CD of 0%, 18%, and 27%.

(b) Comparison curves between 27% and 40%.

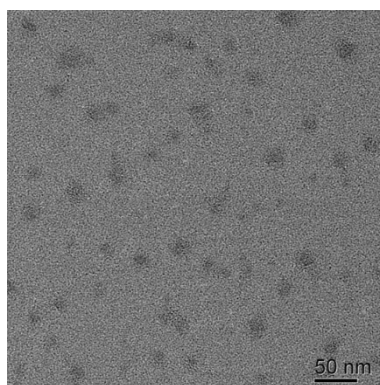


**Figure S6.** TEM image of tadpole-like SCNPs ( $CD_{27\%}$ -P4VP(SCNP) $_{53}$ -*b*-PS $_{569}$ ) prepared in dilute DCM solution.

**Self-assembly behavior of linear BCPs and tadpole-like SCNPs in solution.**

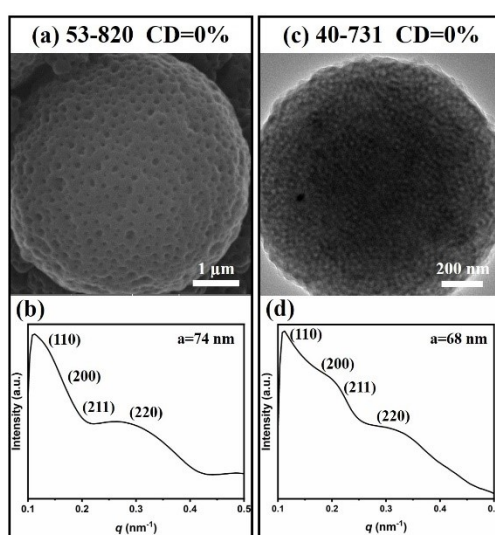


**Figure S7.** Cubosomes obtained by linear P4VP-*b*-PS using DMF as co-solvent. (a, b) SEM image and SAXS pattern of P4VP $_{53}$ -*b*-PS $_{820}$  ( $f_{PS}=94.4\%$ ) ; (c,d) TEM image and SAXS pattern of P4VP $_{40}$ -*b*-PS $_{731}$  ( $f_{PS}=95.2\%$ ).

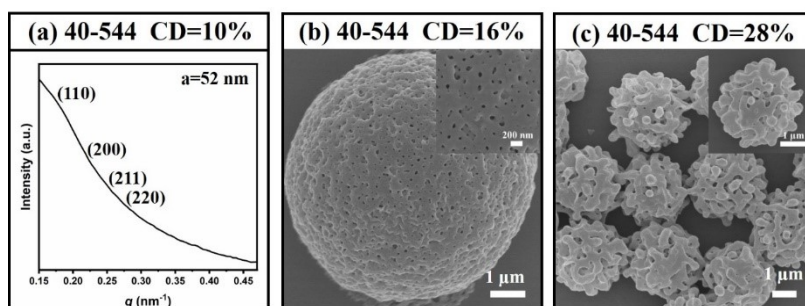


**Figure S8.** (a) SAXS profile of cubosomes formed by  $CD_{10\%}$ -P4VP(SCNP) $_{40}$ -*b*-PS $_{544}$ . SEM images of (b) irregular cubosomes formed by  $CD_{16\%}$ -P4VP(SCNP) $_{40}$ -*b*-PS $_{544}$  and (c) LCMs formed by  $CD_{28\%}$ -P4VP(SCNP) $_{40}$ -*b*-PS $_{544}$  using DMF as co-solvent.

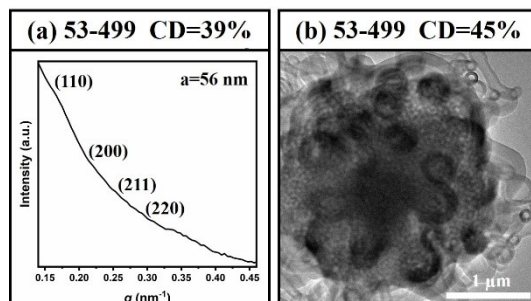


**Figure S9.** (a) SAXS profile of cubosomes formed by  $CD_{39\%}$ -P4VP(SCNP) $_{53}$ -*b*-PS $_{499}$  and (b) TEM image of LCMs with irregular pores and elongated vesicles formed by  $CD_{45\%}$ -P4VP(SCNP) $_{53}$ -*b*-PS $_{499}$  using DMF as co-solvent.

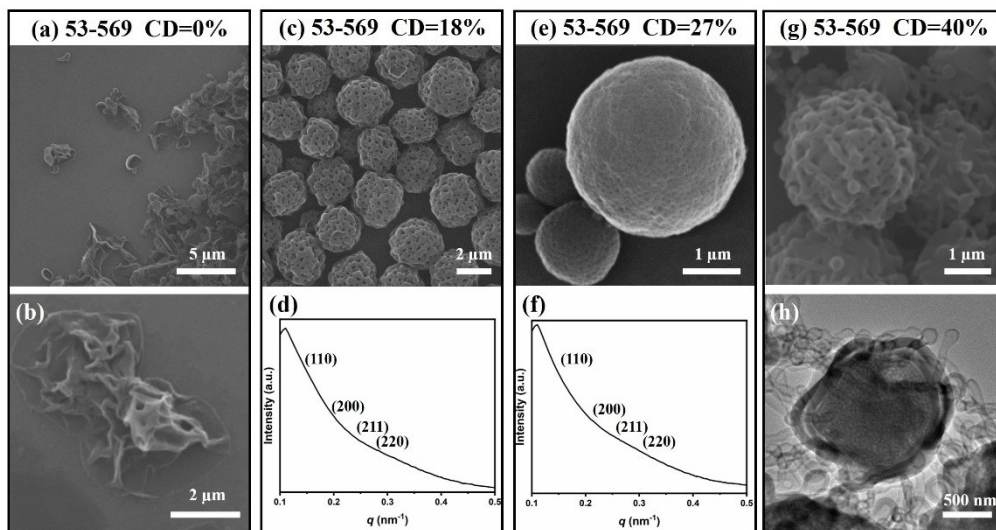


**Figure S10.** (a, b) SEM images of LCVs formed by linear P4VP $_{53}$ -*b*-PS $_{569}$ ; (c, e) SEM images and (d, f) SAXS patterns of cubosomes formed by  $CD_{18\%}$ -P4VP(SCNP) $_{53}$ -*b*-PS $_{569}$  and  $CD_{27\%}$ -P4VP(SCNP) $_{53}$ -*b*-PS $_{569}$ , respectively; (g) SEM image and (h) TEM image of cubosomes with uneven surface formed by  $CD_{40\%}$ -P4VP(SCNP) $_{53}$ -*b*-PS $_{569}$ . All the self-assemblies were obtained by using DMF as co-solvent.



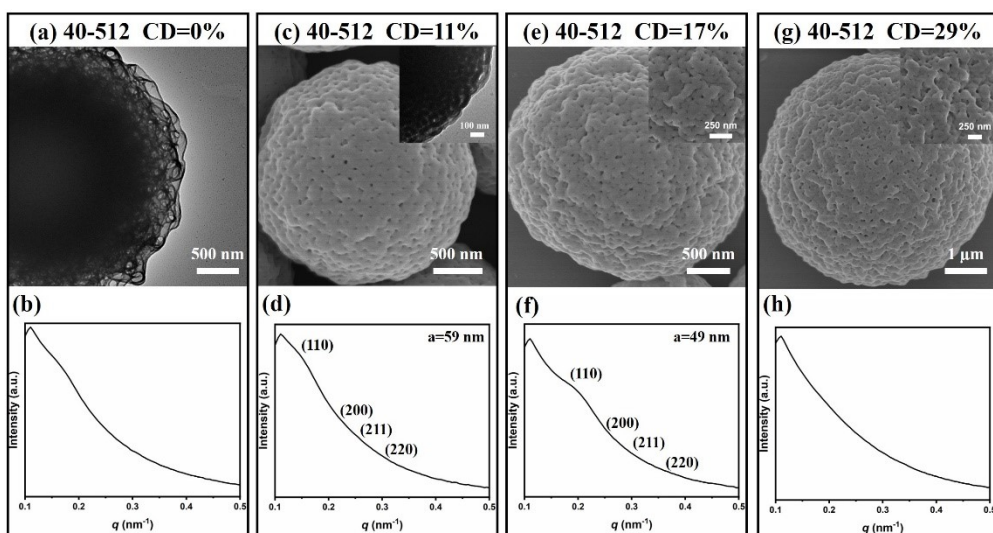


**Figure S11.** (a) TEM image and (b) SAXS pattern of sponges formed by linear P4VP<sub>40</sub>-*b*-PS<sub>512</sub>; (c, e) SEM images (inserts were TEM and SEM image at magnification) and (d, f) SAXS patterns of cubosomes formed by CD<sub>11%</sub>-P4VP(SCNP)<sub>40</sub>-*b*-PS<sub>512</sub> and CD<sub>17%</sub>-P4VP(SCNP)<sub>40</sub>-*b*-PS<sub>512</sub>, respectively; (g) SEM images and (h) SAXS pattern of LCMs formed by CD<sub>29%</sub>-P4VP(SCNP)<sub>40</sub>-*b*-PS<sub>512</sub>. All the self-assemblies were obtained by using DMF as co-solvent.

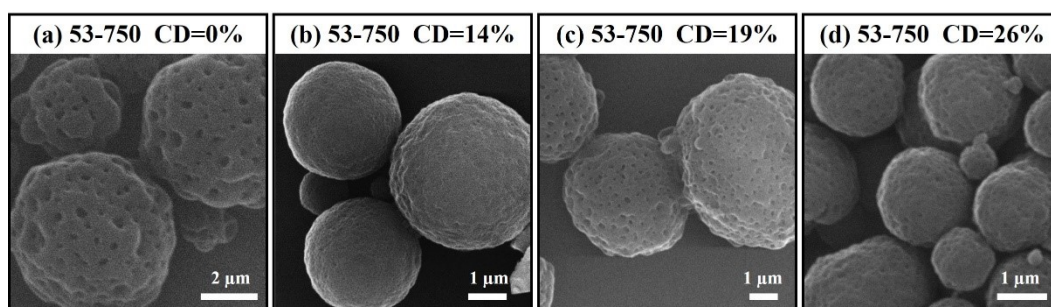


**Figure S12.** SEM images of (a) sponges obtained by linear P4VP<sub>53</sub>-*b*-PS<sub>750</sub>, cubosomes obtained by (b) CD<sub>14%</sub>-P4VP(SCNP)<sub>53</sub>-*b*-PS<sub>750</sub> and (c) CD<sub>19%</sub>-P4VP(SCNP)<sub>53</sub>-*b*-PS<sub>750</sub>, and (d) LCMs obtained by CD<sub>26%</sub>-P4VP(SCNP)<sub>53</sub>-*b*-PS<sub>750</sub> using DMF as co-solvent.

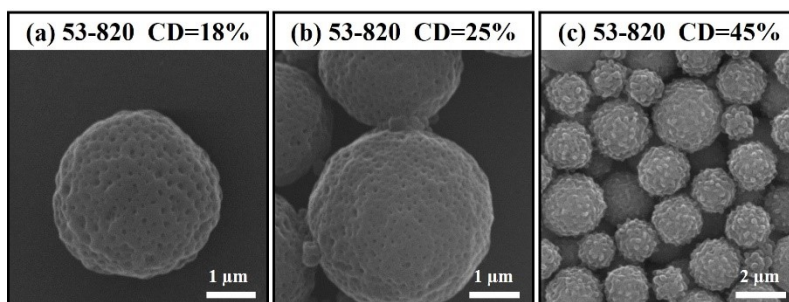


**Figure S13.** SEM images of cubosomes formed by (a) CD<sub>18%</sub>-P4VP(SCNP)<sub>53</sub>-*b*-PS<sub>820</sub> and (b) CD<sub>25%</sub>-

P4VP(SCNP)<sub>53</sub>-*b*-PS<sub>820</sub>, and (c) LCMs formed by CD<sub>45%</sub>-P4VP(SCNP)<sub>53</sub>-*b*-PS<sub>820</sub> using DMF as co-solvent.

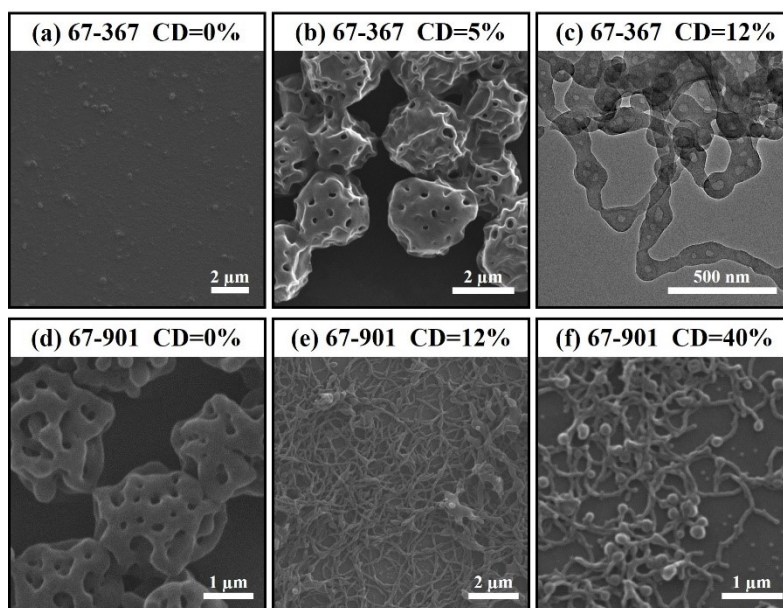


**Figure S14.** SEM images of (a) micelles formed by linear P4VP<sub>67</sub>-*b*-PS<sub>367</sub>, (b) sponges formed by CD<sub>5%</sub>-P4VP(SCNP)<sub>67</sub>-*b*-PS<sub>367</sub>, and (c) nanowires formed by CD<sub>12%</sub>-P4VP(SCNP)<sub>67</sub>-*b*-PS<sub>367</sub> using DMF as co-solvent. SEM images of (d) sponges formed by linear P4VP<sub>67</sub>-*b*-PS<sub>901</sub> and (e, f) nanowires formed by CD<sub>12%</sub>-P4VP(SCNP)<sub>67</sub>-*b*-PS<sub>901</sub> and CD<sub>40%</sub>-P4VP(SCNP)<sub>67</sub>-*b*-PS<sub>901</sub> using DMF as co-solvent.

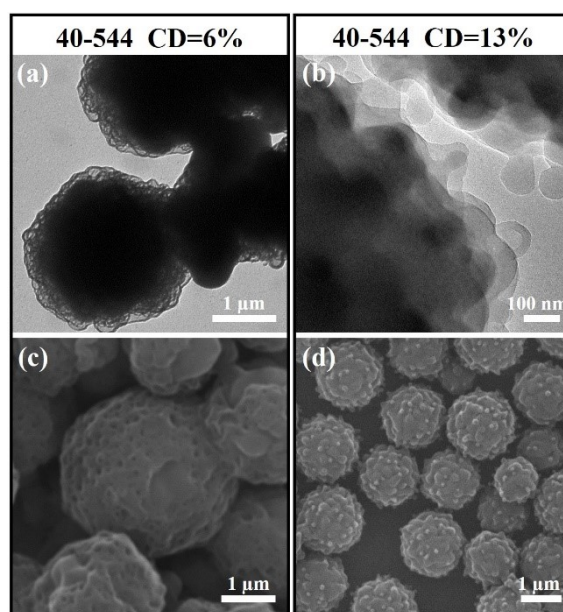


**Figure S15.** SEM and TEM images of (a, c) sponges formed by CD<sub>6%</sub>-P4VP(SCNP)<sub>40</sub>-*b*-PS<sub>544</sub> and (b, d) LCMs with uneven surface formed by CD<sub>13%</sub>-P4VP(SCNP)<sub>40</sub>-*b*-PS<sub>544</sub> using DMF as co-solvent. The

interchain cross-linking nanoparticles were prepared in the dilute dioxane solution.

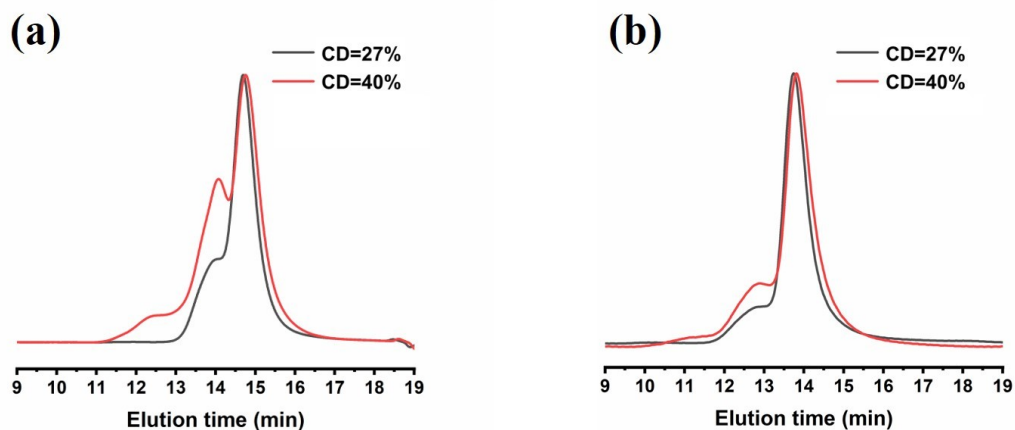


**Figure S16.** GPC traces of P4VP(SCNP)<sub>53</sub>-*b*-PS<sub>569</sub> prepared in dilute DCM solution when CD was 27% and 40%, using (a) DMF and (b) THF as the eluent, respectively.

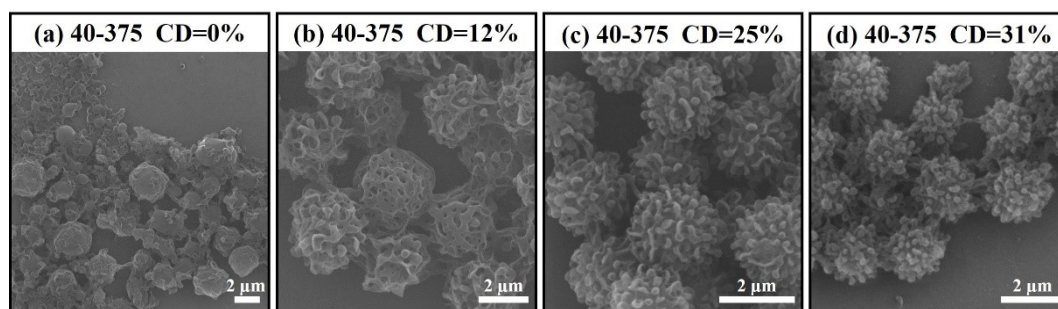


**Figure S17.** SEM images of (a) LCVs formed by linear P4VP<sub>40</sub>-*b*-PS<sub>375</sub>, (b) sponges formed by CD<sub>12%</sub>-P4VP(SCNP)<sub>40</sub>-*b*-PS<sub>375</sub>, and LCMs with uneven surface formed by (c) CD<sub>25%</sub>-P4VP(SCNP)<sub>40</sub>-*b*-PS<sub>375</sub> and (d) CD<sub>31%</sub>-P4VP(SCNP)<sub>40</sub>-*b*-PS<sub>375</sub> using DMF as co-solvent.

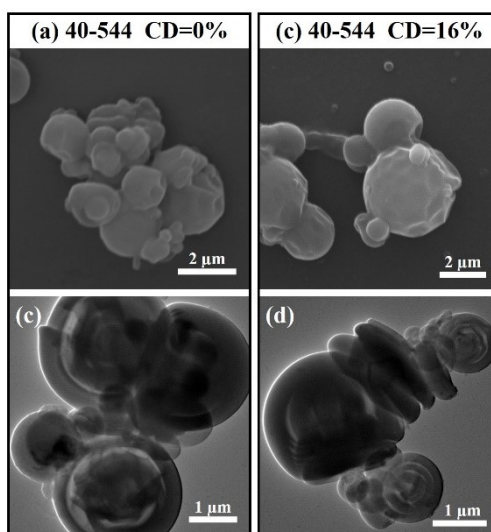


**Figure S18.** SEM and TEM images of LCVs formed by (a, b) linear P4VP<sub>40</sub>-*b*-PS<sub>544</sub> and (c, d) CD<sub>16%</sub>-P4VP(SCNP)<sub>40</sub>-*b*-PS<sub>544</sub> using THF as co-solvent.

**Reference:**

- 1.R. Liu, Z. Rong, G. Han, X. Yang and W. Zhang, *Polymer*, 2021, **215**, 123431.
- 2.Z. Lin, S. Liu, W. Mao, H. Tian, N. Wang, N. Zhang, F. Tian, L. Han, X. Feng and Y. Mai, *Angew. Chem., Int. Ed.*, 2017, **56**, 7135-7140.